MPC based Path Tracking using Potential Field for Autonomous Mobile Robot

Faizudeen Olanrewaju Kajogbola

1 INTRODUCTION

Autonomous Mobile Robots (AMRs) are required to move around to perform some tasks, this makes the ability to navigate effectively and efficiently an important measure of success for any such robot. For navigation, an AMR is required to plan a path leading to its goal point, generate a trajectory along the planned path, and appropriately track such generated trajectory.

Path planning involves searching for an optimal collision-free path from an initial position to some desired goal position which conforms to its physical constraints of the AMR in question [3]. Path planning is divided into: global path planning in which the environment known completely; and the local path planning in which only some section of the environment is known. Common global path planning techniques include A* heuristic search, visibility graph method, generalized Voronoi diagram, ant colony algorithm, genetic algorithm, and the artificial potential field method [10, 16].

The Artificial Potential Field (APF) method draws inspiration from classical physics and was first proposed in 1986 by Khatib [13]. With this method, an AMR seems to move towards its goal position and avoid obstacles instinctively. This is because repulsive potentials are generated to represent obstacles, while attractive potentials are generated to represent the goal position, effectively transforming the path planning problem into an optimization problem [6].

APF approach gives room for the possibility of real-time online path planning. Globally planned paths can be updated with local information from robot sensors- e.g. new location of a moving obstacle, thereby making it possible to plan paths that avoid dynamic obstacles. This, and its mathematical conciseness [16] are some of the reasons why APF-based approaches are widely used in path planning for AMRs. However, if special care is not taken in formulating the potential functions, the robot might get stuck at a local minimum and thereby never reaching its goal position. To prevent this, several methods of formulating the potential functions have been proposed. These include gaussian-shaped repulsive functions [9], the super-quadratic potential function [19], simulated annealing technique [20], and methods that utilize search techniques with the capability of escaping local minima [2].

A trajectory can be generated from a planned path by time parametrization [15]. To enable collision-free navigation, the generated trajectory must respect the dynamical and kinematical constraints of the AMR. Due to nonlinear dynamics, path tracking of AMRs is generally performed using sliding mode control [7], robust control [12], fuzzy logic control [1], or model predictive control (MPC) [6].

In recent years, a lot of research efforts have been poured into implementing MPC algorithms for navigation. Götte et al. in [5] propose a model predictive planning and control (MPPC) approach which handles both trajectory planning and tracking. In [11], Nolte et al. present a generalized approach for path and trajectory planning with model predictive frameworks. A constrained linear time-varying MPC was implemented by Gutjahr et al. in [4] for path tracking and trajectory optimization. While a multi-constrained MPC was presented by Ji et al. in [6] solely for the purpose of path-tracking.

In the following, path tracking and obstacle avoidance for an AMR is investigated. Avoidance of static obstacles in a completely known environment is considered, while taking the robot's kinematic limitations (such as its size, shape, and its steering constraints) into account. An APF approach is used for path planning and trajectory generation, while a multi-constrained model predictive control is used for tracking the generated trajectory. Two MPC controllers are designed, one based on a SISO system model, and the other based on a SIMO model. The performance of the two controllers along with a PID controller are compared under multiple simulation scenarios.

2 PATH PLANNING AND TRAJECTORY GENERATION

This section focuses on path planning and trajectory generation based on Artificial Potential Fields (APFs). While many researchers have proposed a vast array of path planning techniques, APFs pro-

vide an intuitive formulation that allow real-time modifications of planned trajectories. A feature that becomes quite essential in configuration spaces with dynamic obstacles.

The following assumptions are made in this study to simplify the mathematical representation of collision-free trajectories:

- A configuration space of 50m x 50m.
- Static obstacles with rounded geometry of known sizes and positions.
- Constant longitudinal velocity of 1m/s.

2.1 PATH PLANNING

Two coordinate systems are considered. The Autonomous Mobile Robot's (AMR's) body coordinate system $o-xy$, which is centered on the vehicle's center of mass with the x-axis is along the AMR's longitudinal axis, while the y-axis is along it's lateral axis; and a fixed earth coordinate system $O-XY$, which is defined to be colinear with the vehicle body coordinate system at the instant of path planning. At any point in time, the angle of rotation between both coordinate systems is the AMR's yaw angle ψ. The position of the AMR in the fixed-earth coordinate is given as $\vec{X}_r$, the position of the goal point as $\vec{X}_g$, and position of obstacles as $\vec{X}_o$.

The universal potential (U) which guides the AMR to it's goal position is composed of the attractive potential (U_A) and the repulsive potential (U_R).

The attractive potential (U_A) is formulated such that it's minimum point is at the goal position. A mathematical expression for the attractive potential is given as:

$$U_A(\vec{X}_r,\vec{X}_g) := \frac{1}{2}K_{att}\left\|\vec{X}_r-\vec{X}_g\right\|^2$$

where
K_{att} is a constant.
An attractive potential field with AMR initial position $(0,0)$ and goal position $(50,30)$ and $K_{att} = 0.01$ is shown in Figure 1.

The second component of the universal potential is the repulsive potential which results from superimposing the repulsive potential of each obstacle. The repulsive potential of an obstacle has it's peak at the obstacle's position and reduces as the distance from the obstacle increases. It can be expressed as:

$$U_R(\vec{X}_r,\vec{X}_o) := \begin{cases} \frac{1}{2}K_{rep}\left(\frac{1}{\rho}-\frac{1}{\rho_0}\right)^2; & \text{if } \rho<\rho_0 \\ 0; & \text{otherwise} \end{cases}$$

where
$\rho := \left\|\vec{X}_r-\vec{X}_o\right\|$;

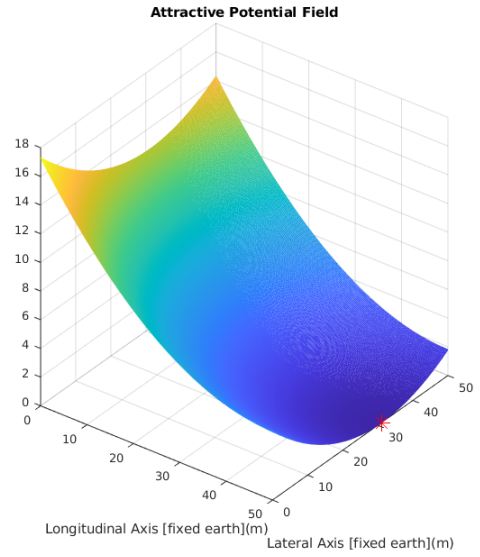

Figure 1: Attractive Potential Field

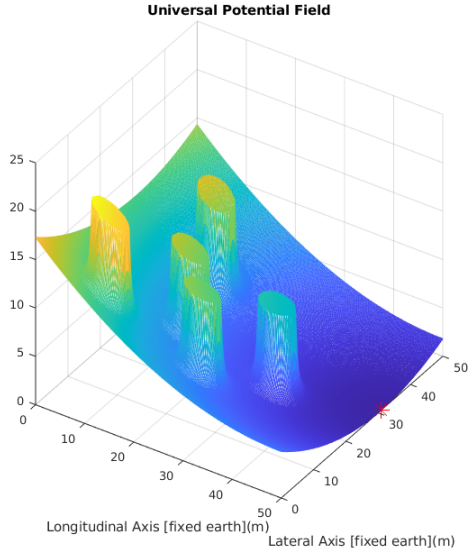

Figure 2: Universal Potential Field

K_{rep} is a constant;
ρ_0 is a constant that dictates the maximum distance from which the influence of an obstacle can be felt. A suitable selection according to kinetic theory is $\rho_0 \geq V_{MAX}/2A_{MAX}$ where V_{MAX} is the maximum speed of the AMR and A_{MAX} is the maximum deceleration of the AMR [14].

Figure 2 shows the universal potential obtained by fusing the attractive potential from Figure 1 with repulsive potentials obtained from circular obstacles of radius $1m$ at coordinates (14.87, 33.28), (10, 8), (26, 12), (19, 19), and (34, 23) with $K_{rep} = 10$.

After setting up the universal potential, a simple gradient descent along this potential yields a "force" that guides the AMR towards the goal position while deflecting it away from the obstacles.

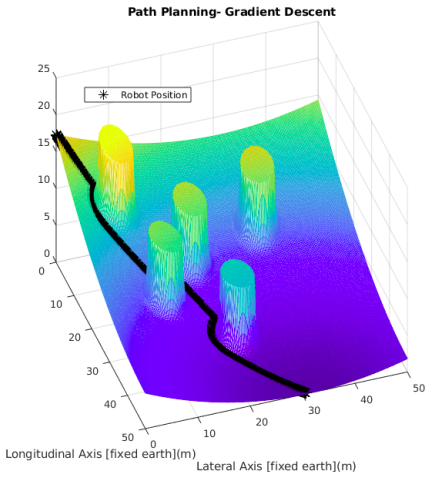

Figure 3: Gradient descent along Universal Potential Field

This force can be interpreted as the velocity vector of the AMR along the planned path, and can be expressed as:

$$F := F_A + F_R$$

where F_A is the attractive force which is given by:

$$F_A(\vec{X}_r, \vec{X}_o) := -grad(U_A)$$

$$F_A(\vec{X}_r, \vec{X}_o) = -K_{att}\left(\vec{X}_r - \vec{X}_g\right)$$

and F_R is the repulsive force which is given by:

$$F_R(\vec{X}_r, \vec{X}_o) := \sum_{\vec{X}_o \in \Omega} -grad(U_R)$$

$$-grad(U_R) = \frac{K_{rep}}{\rho^3}\left(\frac{1}{\rho} - \frac{1}{\rho_0}\right)\left(\vec{X}_r - \vec{X}_o\right)$$

where $\rho = \left\|\vec{X}_r - \vec{X}_o\right\|$;
Ω is a set of all obstacle coordinates.

Building upon the universal potential depicted in Figure 2, Figure 3 shows the resulting collision-free path from the AMR's initial position (0, 0) to a goal position of (50, 30).

2.2 TRAJECTORY GENERATION

A planned path can be transformed into a trajectory by time-parametrizing it [15]. Following from our earlier assumption of the AMR having a constant velocity of $1m/s$, we can generate a trajectory from our planned path by simulating forward in time along the planned path with a velocity vector of magnitude $1m/s$.

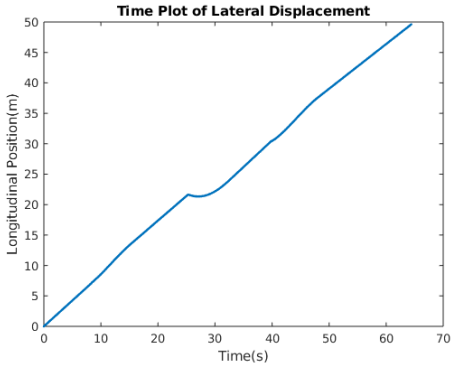

Figure 5: Trajectory Generation- Longitudinal Displacement

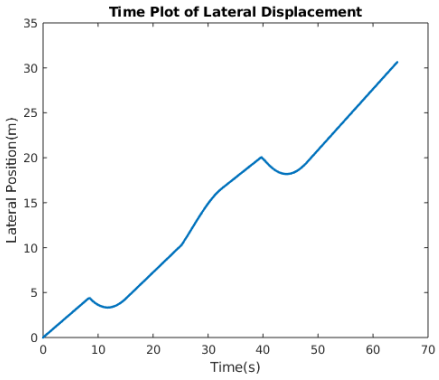

Figure 4: Trajectory Generation- Lateral Displacement

Figures 4 and 5 show the trajectory information for the path illustrated in Figure 3 simulated with a sampling time of 0.1 seconds.

3 MATHEMATICAL MODEL FOR PATH TRACKING PROBLEM

The mathematical model used for MPC design is described in this section. Since the success of any controller design is highly dependent on the accuracy of the plant model employed, correct modelling of the AMR is necessary. While the dynamics of AMRs are generally nonlinear, MPC allows us to base our design on a linearized model and still get satisfactory results.
For the path tracking problem considered in this paper, the following simplifying assumptions are made:

- The AMR is a front wheel controller vehicle with a single front wheel and two rear wheels.
- Motion is only in the X-Y plane, i.e. rolling and pitching motions are ignored.
- Model parameters are constant.

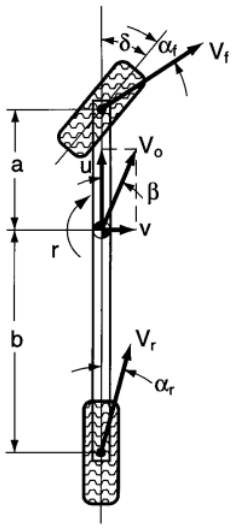

Figure 6: 2 DOF Bicycle Model [8]

- The AMR is operating in an indoor environment with a smooth and flat surface, such that gravitational and aerodynamic side forces can be ignored.
- Constant longitudinal velocity with perfect tracking along the longitudinal axis.

3.1 DYNAMICAL MODEL FOR LATERAL PATH TRACKING

With the above assumptions, and also by lumping the two rear wheel into a single wheel, the linear two degree of freedom bicycle model (shown in FIgure 6) of a conventional vehicle can be employed.
Considering Newton's law of conservation of momentum along the lateral-axis, we have:

$$F_{xf}cos(\delta)+F_{xr}=m(\dot{u}-\dot{\psi}v)$$
$$aF_{xf}cos(\delta)-bF_{xr}=I_{zz}\dot{r}$$

Front tyre slip angle

$$\gamma_f = atan\left(\frac{u+a\dot{\psi}}{v}\right)-\delta$$

Rear tyre slip angle

$$\gamma_r = atan\left(\frac{u-b\dot{\psi}}{v}\right)$$

Front tyre lateral force

$$F_{xf}=C_f\gamma_f$$

Rear tyre lateral force

$$F_{xr}=2C_r\gamma_r$$

Sideslip angle

$$\beta = atan\left(\frac{u}{v}\right)$$

With small angles approximations, the sideslip angle can be approximated as

$$\beta=\frac{u}{v}$$

The front tyre angle as

$$\gamma_f=\frac{u+a\dot{\psi}}{v}-\delta=\beta+\frac{a\dot{\psi}}{v}+\delta$$

And the rear tyre angle as

$$\gamma_r=\frac{u-b\dot{\psi}}{v}=\beta-\frac{b\dot{\psi}}{v}$$

The equations of motion then yield the following differential equations:

$$\dot{\beta}=-\frac{\beta}{mv}\left(C_f+2C_f\right)+r\left[\frac{1}{mv^2}\left(2bC_r-aC_f\right)\right]+\delta\frac{C_f}{mv}$$

$$\dot{r}=-\frac{\beta}{I_{zz}}\left(aC_f-2bC_r\right)-r\left[\frac{1}{I_{zz}v}\left(a^2C_f+2b^2C_r\right)\right]+\delta\frac{aC_f}{I_{zz}}$$

By selecting the state variables:

- Lateral displacement of CoM, x_c
- Side-slip angle, β
- Yaw angle, ψ
- Yaw velocity, r

The following state space representation of the system is obtained

$$\begin{bmatrix}\dot{x_c}\\ \dot{\beta}\\ \dot{\psi}\\ \dot{r}\end{bmatrix}=\begin{bmatrix}0 & v & v & 0\\ 0 & -\frac{C_f+2C_r}{mv} & 0 & \frac{2bC_r-aC_f}{mv^2}-1\\ 0 & 0 & 0 & 1\\ 0 & \frac{2bC_r-aC_f}{I_{zz}} & 0 & -\frac{\left(2b^2C_r+a^2C_f\right)}{I_{zz}v}\end{bmatrix}\begin{bmatrix}x_c\\ \beta\\ \psi\\ r\end{bmatrix}+\begin{bmatrix}0\\ \frac{C_f}{mv}\\ 0\\ \frac{aC_f}{I_{zz}}\end{bmatrix}\delta$$

3.1.1 SISO Model

For the first MPC controller, the lateral position of the AMR in the fixed earth coordinate system $O-XY$ only is selected as the system output. The output equation is then

$$x_c=\begin{bmatrix}1 & 0 & 0 & 0\end{bmatrix}\begin{bmatrix}x_c\\ \beta\\ \psi\\ r\end{bmatrix}$$

3.1.2 SIMO Model

For the second MPC controller, the yaw angle is also selected as an output, such that the output equation becomes

$$\begin{bmatrix} x_c \\ \psi \end{bmatrix} = \begin{bmatrix} 1 & 0 & 0 & 0 \\ 0 & 0 & 1 & 0 \end{bmatrix} \begin{bmatrix} x_c \\ \beta \\ \psi \\ r \end{bmatrix}$$

4 CONTROLLER DESIGN

Three different controllers are designed during the course of this study. While the main focus is on model predictive control (MPC), a PID controller is also designed for comparative study.

4.1 MPC CONTROLLER DESIGN

Model predictive control has risen in popularity in both research and industry in recent years. This can mainly be attributed to rapid advances in computing technologies. Of all its pros, MPC is considered in this study largely because it allows embedding model constraints in the controller. This makes it possible to specify rate and limit constraints on the control signal (front wheel steering angle). Two MPC controllers are designed, one based on the SISO model and the other based on the SIMO model of the AMR. For the SIMO-based MPC controller, the two outputs are equally punished (i.e. deviations from the reference the lateral displacement has an equally weighted effect on the optimization cost function as deviations from the reference yaw angle). The MPCs are designed using the Model Predictive Controller model from Simulink's Model Predictive Control Toolbox [17].

MPC Parameters:

- Prediction horizon: 25 time-steps
- Control horizon: 4 time-steps

MPC Output Constraints:

- Maximum front wheel steering angle: $\pm 40\,\text{deg}$
- Maximum front wheel angular velocity: $\pm 40\,\text{deg}$

5 SIMULATION

Extensive simulation is carried out to examine the effects of the designed controllers on a representative model of the Autonomous Mobile Robot (AMR). The Vehicle Body 3DOF Single Track model from Simulink's Vehicle Dynamics Blockset which implements a rigid two-axle vehicle body model to calculate longitudinal, lateral, and yaw motion is used for simulation [18]. This model is sufficient for modelling non-holonomic vehicle motion when vehicle pitch, roll, and vertical motion are not significant which is the case in this study.

In all simulation scenarios, perfect tracking of the AMR's longitudinal position is assumed since this study focuses on lateral displacement control. Hence, the reference signal is the lateral position trajectory generated by the Artificial Potential Field (APF) path planning algorithm. In addition to the lateral position reference, the yaw angle reference is also provided as reference for the SIMO-based MPC.

Performance of the controllers are compared on the basis of a scaled error norm, which is the L2 norm of the error at each sampling instance divided by the number of samples.

5.1 PARAMETERS

5.1.1 Path Planning

An indoor environment with smooth and flat surface of 50mx50m is assumed, making it possible to ignore gravitation and aerodynamic side forces. Also, static rounded obstacles are implemented at various locations in the simulation environment. The following path planning parameters are used in simulation:

- Attractive potential constant, K_{att}: 0.01
- Repulsive potential constant, K_{rep}: 10
- Obstacle radius: $1m$
- Obstacle locations: $(14.87, 33.28)$; $(10.00, 8.00)$; $(26.00, 12.00)$; $(19.00, 19.00)$; and $(34.00, 23.00)$
- AMR size allowance: $0.35m$
- AMR initial position: $(0, 0)$
- AMR goal position: $(50, 31)$

5.1.2 AMR

The AMR is modelled as a scaled down version of a conventional car. A single front wheel and two rear wheels are assumed. The following parameters are used in simulating the AMR:

- Mass: $505kg$
- Yaw mass moment of inertia: $808.5kg.m^2$
- Distance of front wheel from center of mass: $0.3500m$
- Distance of rear wheels from center of mass: $0.4125m$

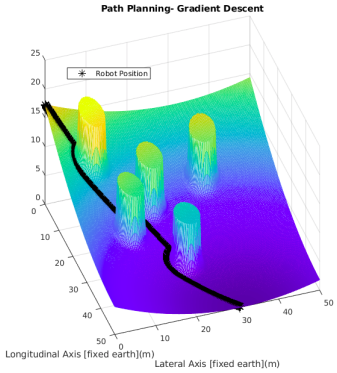

Figure 7: Scenario 1: Path Planning

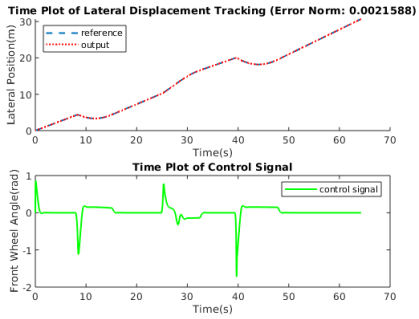

Figure 8: Scenario 1: Lateral Displacement Tracking with PID Controller

5.1.3 Others

- Sampling time (PID Controller): $0.01s$
- Sampling time (MPC Controllers): $0.05s$

5.2 SIMULATION SCENARIO 1

The simulation environment is setup as described in Section 5.1.1 and Figure 7 shows the universal potential field and the planned path.

Simulation is carried out using each of the 3 controllers, and their performances compared using the scaled error norm which is evaluated as an L2 norm of the lateral displacement tracking error divided by the number of time-steps.

The PID controller is able to guide the system along the planned path best, yielding a scaled error norm of 0.0022 (Figure 8) albeit with a rather high peak control signal (front wheel steering angle) of about $-1.5rad \approx -85.94$ deg which is not possible for typical wheel setups. The SIMO-based MPC performs a little better than the SISO-based MPC with error norms of 0.3647 (Figure 9) and 0.4714 (Figure 10) respectively. Both yielding control signals within the specified constraints of ± 40 deg.

Motion of the AMR through the simulation environment as controlled by the PID, SIMO-based MPC, and SISO-based MPC are shown in Figures 11, 13, and 12 respectively.

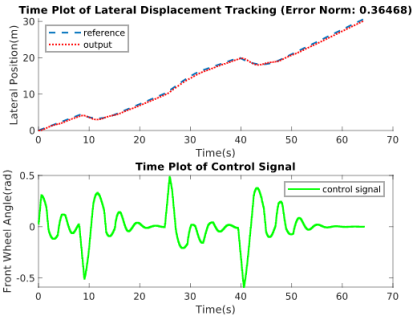

Figure 9: Scenario 1: Lateral Displacement Tracking with SIMO MPC

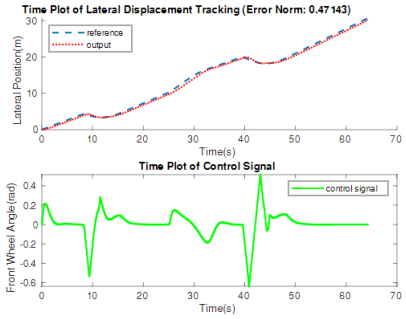

Figure 10: Scenario 1: Lateral Displacement Tracking with SISO MPC

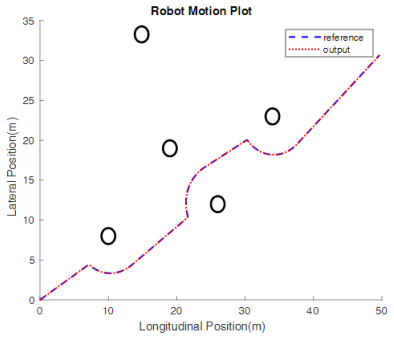

Figure 11: Scenario 1: AMR Motion in Simulation Environment for PID Controller

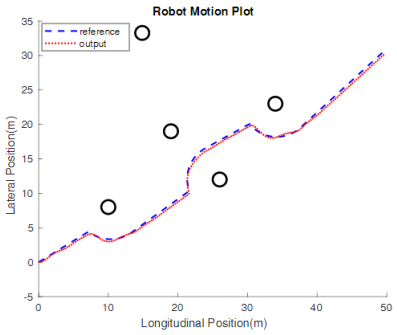

Figure 12: Scenario 1: AMR Motion in Simulation Environment for SIMO MPC

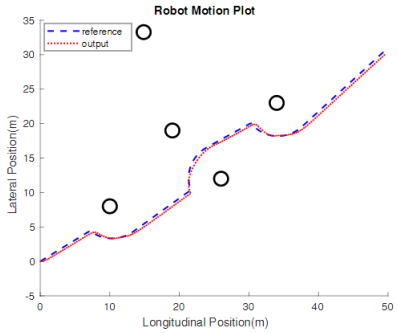

Figure 13: Scenario 1: AMR Motion in Simulation Environment for SISO MPC

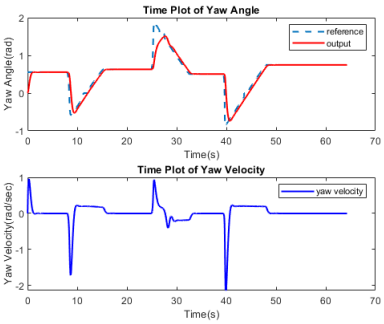

Figure 14: Scenario 1: Yaw Angle and Yaw Velocity resulting from PID Controller

The resulting yaw angles and yaw velocities from the PID controller, SIMO-based MPC, and SISO-based MPC are exhibited in Figures 14, 15, and 16 respectively.

In conclusion, we can infer that the PID controller performed best, it would require some special wheel setup to pull off about 90 deg wheel angle. Further, the better performance of the SIMO-based MPC than the SISO-based MPC may be attributed to the extra yaw angle information available to the SIMO-based MPC.

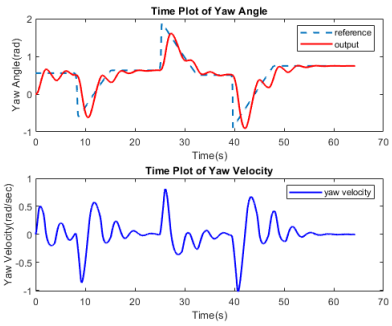

Figure 15: Scenario 1: Yaw Angle and Yaw Velocity resulting from SIMO MPC

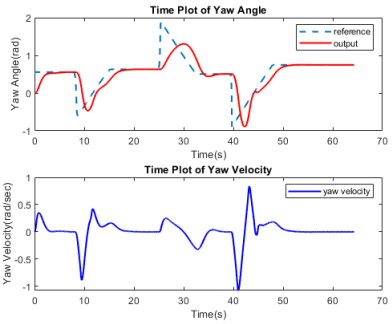

Figure 16: Scenario 1: Yaw Angle and Yaw Velocity resulting from SISO MPC

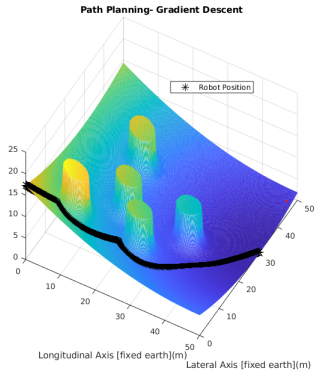

Figure 17: Scenario 2: Path Planning

5.3 SIMULATION SCENARIO 2

As opposed to that of the simulation environment setup as described in Section 5.1.1, Figure 17 shows the universal potential field and the planned path.

Although the PID controller gives the lowest scaled error norm of 0.0044 (Figure 18), the control signal (front wheel steering angle) it produces is very unrealistic. The control signal rises up to about $-5.35 rad \approx -306.53$ deg at some point.

The SIMO-based MPC is the controller of choice in this scenario, with a scaled error norm of 0.400

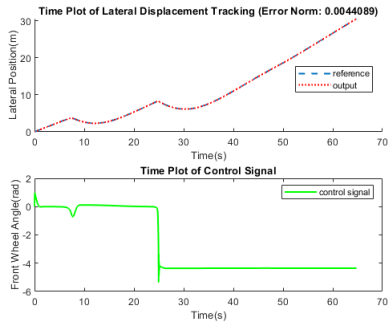

Figure 18: Scenario 2: Lateral Displacement Tracking with PID Controller

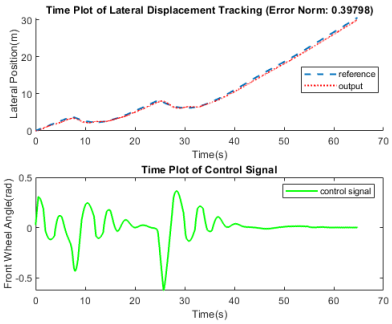

Figure 19: Scenario 2: Lateral Displacement Tracking with SIMO MPC

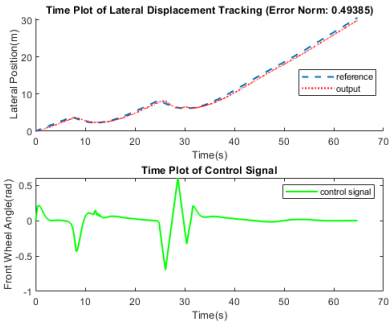

Figure 20: Scenario 2: Lateral Displacement Tracking with SISO MPC

(Figure 24).

The SISO-based MPC produced the largest scaled error norm of 0.4939 (Figure 20). Both yielding control signals within the specified constraints of $\pm 40\,\text{deg}$.

Motion of the AMR through the simulation environment as controlled by the PID, SIMO-based MPC, and SISO-based MPC are shown in Figures 21, 23, and 25 respectively.

In conclusion, we can infer that while the PID controller cannot be implemented in this scenario. Rather, the SIMO-based MPC should be used.

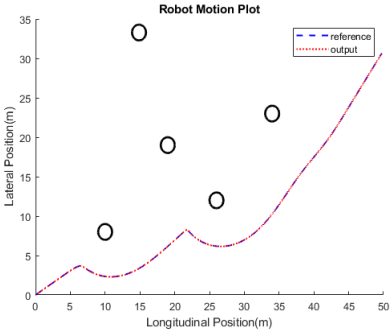

Figure 21: Scenario 2: AMR Motion in Simulation Environment for PID Controller

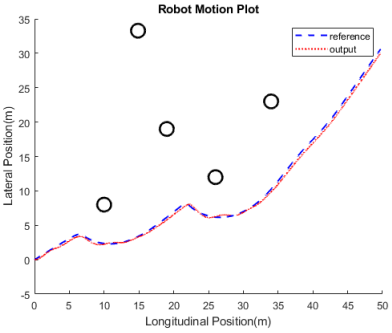

Figure 22: Scenario 2: AMR Motion in Simulation Environment for SIMO MPC

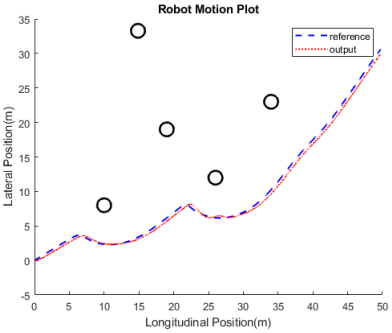

Figure 23: Scenario 2: AMR Motion in Simulation Environment for SISO MPC

5.4 SIMULATION SCENARIO 3

The simulation environment is setup as described in Section 5.1.1 however, an error is introduced such that the initial position of the AMR as seen by the path planning algorithm is $(0,0)$, while the initial position of the AMR in simulation is actually $(0,1)$. For this scenario, only the performance of the MPC controllers are evaluated. Figure 7 shows the universal potential field and the planned path which remains the same as from scenario 1.

The SIMO-based MPC is able to overcome this initial error and guide the AMR onto the planned path as evident in Figures 24 and 25. However looking at Figure 26 shows that the SISO-based

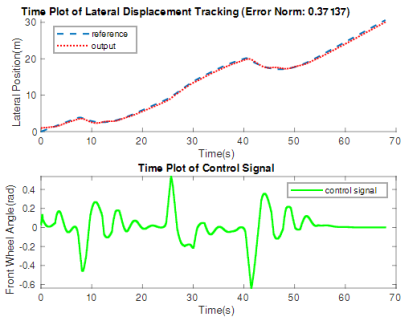

Figure 24: Scenario 3: Lateral Displacement Tracking with SIMO MPC

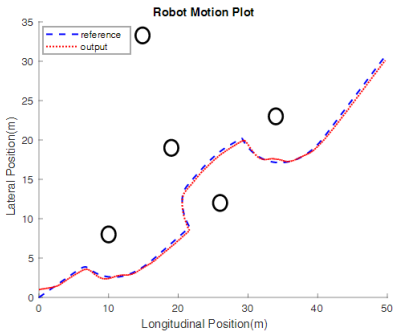

Figure 25: Scenario 3: AMR Motion in Simulation Environment for SIMO MPC

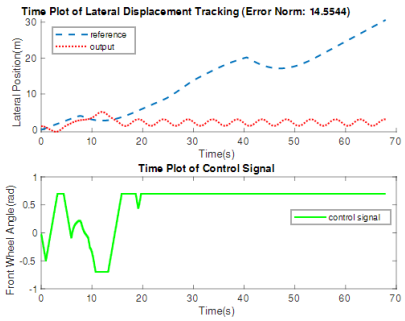

Figure 26: Scenario 3: Lateral Displacement Tracking with SISO MPC

MPC is unable to do so. Instead, lateral control of the AMR becomes unstable and as a result, the AMR starts going in circles as can be seen in Figure 27. For this behavior to be visualized, the assumption of perfect longitudinal tracking is revoked.

The prediction horizon of the SISO-based MPC is increased from 25 time-steps to 35 time-steps to enable it predict the behavior of the AMR further in time. The results of simulation with this increase are displayed in Figures 28 and 29 . With a prediction horizon of 35 time-steps, the SISO-based MPC is also able to overcome the initial error and guide the AMR onto the planned path.

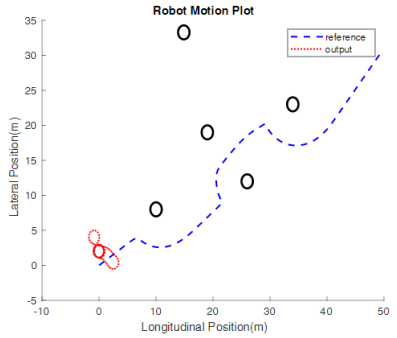

Figure 27: Scenario 3: AMR Motion in Simulation Environment for SISO MPC

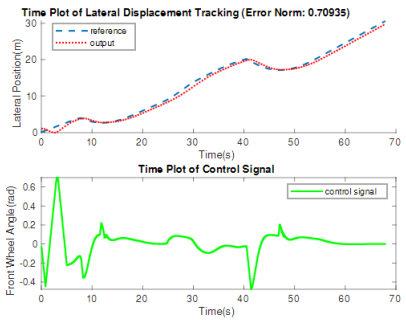

Figure 28: Scenario 3: Lateral Displacement Tracking with SISO MPC with extended Prediction Horizon

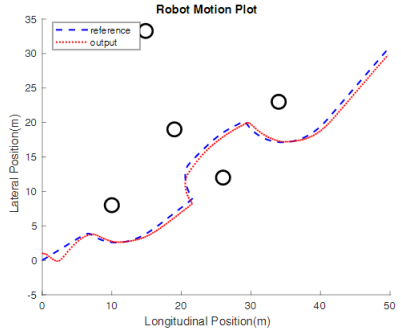

Figure 29: Scenario 3: AMR Motion in Simulation Environment for SISO MPC with extended Prediction Horizon

6 CONCLUSION

In an indoor environment with an accurate mapping and localization scheme, path planning and obstacle avoidance for Autonomous Mobile Robots moving at an average velocity can be successfully carried out using an Artificial Potential Field based approach and Model Predictive Control.

REFERENCES

[1] G. Antonelli, S. Chiaverini, and G. Fusco. A fuzzy-logic-based approach for mobile robot path tracking. *IEEE Transactions on Fuzzy Systems*, 15(2):211–221, April 2007.

[2] J. Barraquand, B. Langlois, and J. . Latombe. Numerical potential field techniques for robot path planning. *IEEE Transactions on Systems, Man, and Cybernetics*, 22(2):224–241, March 1992.

[3] Z. X. Cai, H. G. He, and H. Chen. Some issues for mobile robots navigation under unknown environments. In *Proc. IEEE Internation Conference on Decision and Control*, volume 17, pages 385–390, 2002.

[4] B. Gutjahr, L. Gröll, and M. Werling. Lateral vehicle trajectory optimization using constrained linear time-varying mpc. *IEEE Transactions on Intelligent Transportation Systems*, 18(6):1586–1595, June 2017.

[5] C. Götte, M. Keller, C. Rösmann, T. Nattermann, C. Haß, K. Glander, A. Seewald, and T. Bertram. A real-time capable model predictive approach to lateral vehicle guidance. In *2016 IEEE 19th International Conference on Intelligent Transportation Systems (ITSC)*, pages 1908–1913, Nov 2016.

[6] J. Ji, A. Khajepour, W. W. Melek, and Y. Huang. Path planning and tracking for vehicle collision avoidance based on model predictive control with multiconstraints. *IEEE Transactions on Vehicular Technology*, 66(2):952–964, Feb 2017.

[7] Jong-Min Yang and Jong-Hwan Kim. Sliding mode control for trajectory tracking of nonholonomic wheeled mobile robots. *IEEE Transactions on Robotics and Automation*, 15(3):578–587, June 1999.

[8] J. Kiefer. Modeling of road vehicle lateral dynamics, 1996.

[9] D. Koditschek. Exact robot navigation by means of potential functions: Some topological considerations. In *Proceedings. 1987 IEEE International Conference on Robotics and Automation*, volume 4, pages 1–6, March 1987.

[10] V. Kunchev, L. Jain, V. Ivancevic, and A. Finn. Path planning and obstacle avoidance for autonomous mobile robots: A review. In *Knowledge-Based Intelligent Information and Engineering Systems*, volume 4252, pages 537–544. Springer, Berlin, Heidelberg, 2006.

[11] M. Nolte, M. Rose, T. Stolte, and M. Maurer. Model predictive control based trajectory generation for autonomous vehicles — an architectural approach. In *2017 IEEE Intelligent Vehicles Symposium (IV)*, pages 798–805, June 2017.

[12] Julio E. Normey-Rico, Ismael Alcalá, Juan Gómez-Ortega, and Eduardo F. Camacho. Mobile robot path tracking using a robust pid controller. *Control Engineering Practice*, 9(11):1209 – 1214, 2001. PID Control.

[13] Khatib Oussama. *The Potential Field Approach And Operational Space Formulation In Robot Control*, pages 367–377. Springer US, Boston, MA, 1986.

[14] S. M. H. Rostami, A. K. Sangaiah, J. Wang, and X. Liu. Obstacle avoidance of mobile robots using modified artificial potential field algorithm. *EURASIP Journal on Wireless Communications and Networking*, 2019(70), 2019.

[15] Christoph Rösmann, Wendelin Feiten, Thomas Wösch, Frank Hoffmann, and Torsten Bertram. Trajectory modification considering dynamic constraints of autonomous robots. In *Proc. of ROBOTIK 2012- 7th German Conference on Robotics*, pages 74–79, 2012.

[16] P. Shi and Y. W. Zhao. An efficient path planning alogrithm for mobile robot using improved potential field. In *Proc. IEEE Int. Conference ROBIO*, volume 1-4, pages 1704–1708, 2009.

[17] Inc. The MathWorks. *Simulate Model Predictive Controller- Model Predictive Control Toolbox*, 2020 (accessed June 26, 2020).

[18] Inc. The MathWorks. *Vehicle Body 3DOF- Vehicle Dynamics Blockset*, 2020 (accessed June 26, 2020).

[19] R. Volpe and P. Khosla. Manipulator control with superquadric artificial potential functions: theory and experiments. *IEEE Transactions on Systems, Man, and Cybernetics*, 20(6):1423–1436, Nov 1990.

[20] Q. Zhu, Y. Yan, and Z. Xing. Robot path planning based on artificial potential field approach with simulated annealing. In *Sixth International Conference on Intelligent Systems Design and Applications*, volume 2, pages 622–627, Oct 2006.